Journal of
Mechanical
Science and
Technology

Journal of Mechanical Science and Technology 21 (2007) 1541~1547

Research on interactive influences of parameters on T-shaped cold ring rolling by 3d-FE numerical simulation

Lanyun Li, He Yang*, Lianggang Guo, Zhichao Sun

College of Materials Science and Engineering, Northwestern Polytechnical University, Xi'an 710072, P. R. China

(Manuscript Received May 31, 2007; Revised August 30, 2007; Accepted September 30, 2007)

Abstract

Cold ring rolling is a much complex physical process with multi-factors. Two forming parameters, the feed rate of mandrel and the rotational speed of main roll, affect the quality of deformed ring significantly and the feed amount per revolution of ring in the form of their ratio. By their ratio, the interactive effects of the two forming parameters on the T-shaped cold ring rolling process are explored through 3D-FEM in Abaqus software. The results show: firstly the study objects (roll force, growth rate of diameter, degree of inhomogeneous deformation, filling capability of groove, average side spread and fishtail coefficient) are almost invariable if the two parameters are increased (or decreased) proportionally; secondly whether the ratio is changed by the feed rate of mandrel or by the rotational speed of main roll, the variation of each study object with the ratio is approximately the same; thirdly the increase of the ratio is beneficial to the growth of diameter and the restrictions of inhomogeneous deformation, average side spread and fishtail coefficient, but it causes the roll force to increase and the filling capability of groove to decrease.

Keywords: Cold ring rolling process; Feed rate of mandrel; Rotational speed of main roll; Abaqus

1. Introduction

Cold ring rolling is an advanced continuous and local deforming process to manufacture seamless ring parts. The research and development of precise cold ring rolling technology has become an important subject in advanced plastic processing field. During the process (as shown in Fig. 1), the rotation of main roll drives the ring blank through the roll gap, which is decreasing all along due to the advancing mandrel. It can be seen that the two important forming parameters, f and n_1, affect interactively the metal forming state in the roll gap. In order to further reveal the deformation mechanism of cold ring rolling process, it is necessary to investigate the interactive effects of f and n_1 on the process. However, much research on the ring rolling process was carried out by experiments [1], theories [2-3] and finite techniques [4-7] during the past years. Very little attention was paid to this field. And due to the complexity of the process, it is obviously difficult to deeply understand the process purely by using analytical and experimental methods.

Therefore, in this study, the flowchart of Δh, which is the key factor of metal forming state in the roll gap, is built first. It is found that Δh is affected by f and n_1 in the form of f/n_1. Then, by using the 3D-FEM, Abaqus, the interactive effects of f and n_1 on the T-shaped cold ring rolling process are investigated from the following three aspects in terms of $\bar{f}$ ($\bar{f} = f/n_1$).

(1) The variations of RF, $\Delta\dot{R}$, φ_{id}, S, $\bar{B}$ and FT when f and n_1 are increased proportionally to keep $\bar{f}$ unchanged;

*Corresponding author. Tel.: +86 29 884 95632, Fax.: +86 29 884 95632
E-mail address: lanyun7810@126.com

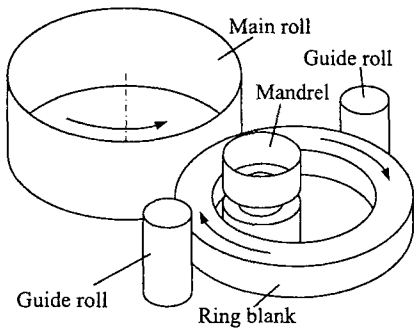

Fig. 1. Sketch of ring rolling process.

(2) The variations of RF, $\Delta\dot{R}$, φ_{id}, S, $\bar{B}$ and FT with $\bar{f}$ when $\bar{f}$ is changed by f but n_1 is unchanged;

(3) The variations of the same objects when $\bar{f}$ is changed by n_1 but f is unchanged.

2. Flowchart of feed amount per revolution of ring

Assuming that the ring blank just rotates N revolutions when the cold ring rolling process is completed, we can get

$$\Delta h_i = f \cdot \Delta t_i = f \cdot \frac{2\pi R_{i-1}}{v_R}, (i = 1,2,3,\cdots,N). \quad (1)$$

$$H_i = H_{i-1} - \Delta h_i = H_0 - \sum_{j=1}^{i} \Delta h_j, (i = 1,2,3,\cdots,N). \quad (2)$$

Assuming no slippage between the ring blank and main roll, we can obtain that v_R is equal to v_D, i.e.,

$$v_R = v_D = 2\pi \cdot n_1 \cdot R_D, (i = 1,2,3,\cdots,N). \quad (3)$$

Substituting Eq. (3) into Eq. (1), we can have

$$\Delta h_i = \frac{R_{i-1}}{R_D} \cdot \frac{f}{n_1}, (i = 1,2,3,\cdots,N). \quad (4)$$

Assuming no side spread and volume constancy in cold ring rolling operation, we can have

$$\pi(R_i^2 - r_i^2) = \pi(R_0^2 - r_0^2), (i = 1,2,3,\cdots,N). \quad (5)$$

$$r_i = R_i - H_i, (i = 1,2,3,\cdots,N). \quad (6)$$

$$H_0 = R_0 - r_0. \quad (7)$$

$$R_i = \frac{1}{2}\left[(R_0 + r_0)\frac{H_0}{H_i} + H_i\right], (i = 1,2,3,\cdots,N). \quad (8)$$

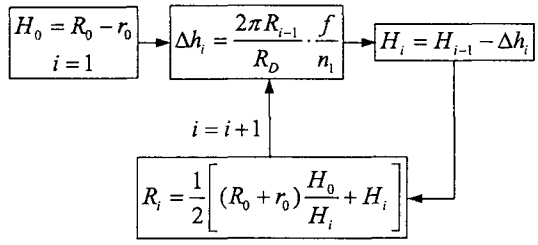

Fig. 2. Flowchart for Δh_i.

According to Eqs. (2), (4), (7) and (8), the flowchart for calculating Δh_i can be obtained, as shown in Fig. 2. It can be seen obviously that f and n_1 affect Δh_i in the form of f/n_1. In order to conveniently investigate the interactive influences of f and n_1 on the cold ring rolling process, the ratio of f to n_1, which is marked as $\bar{f}$, is introduced into this study.

3. 3D-FE model of cold ring rolling process and determination of the range of $\bar{f}$ for modeling

3.1 3D-FE model of cold ring rolling

The authors have built a 3D-FE model of cold ring rolling in Abaqus software as shown in Fig. 3. In the model, the main roll, mandrel and guide rolls are treated as rigid bodies. The guide rolls are controlled by the hydraulic adjustment mechanism, so the problem of guide roll control in ring rolling process with complicated section ring is solved. For T-shaped ring rolling process, the mesh density around the groove is considered higher to improve the deformation accuracy in this area. The model has been validated with respect to the side spread in plane ring rolling process and cross-sectional configuration of deformed ring in T-shaped ring rolling process [9].

The material of ring blank used in the model is A-alloy HE30. Its density, Young modulus and Poisson ratio are 2700kg/m^3, 69GPa and 0.33, respectively, and the constitutive equation is as follows [4].

$$\begin{cases} \bar{\sigma} = 69\bar{\varepsilon}^e (\text{GPa}) & \bar{\varepsilon} \le 0.003 \\ \bar{\sigma} = 231.6(1.0 + 3001.8\bar{\varepsilon}^p)^{0.0653} (\text{MPa}) & \bar{\varepsilon} > 0.003 \end{cases}$$

where $\bar{\sigma}$ is the true stress, $\bar{\varepsilon}^e$ and $\bar{\varepsilon}^p$ are the true elastic and plastic strain, respectively, and $\bar{\varepsilon}$ is the true total strain.

The outer and inner radii and axial width of ring blank are 63.5, 38.1 and 25.4 mm, respectively. The

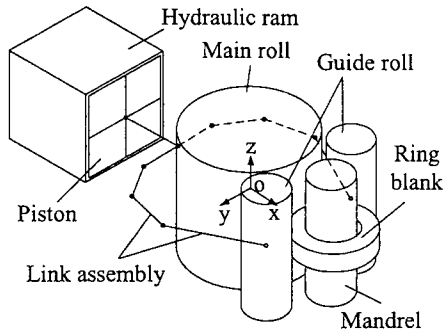

Fig. 3. 3D-FE model of cold ring rolling.

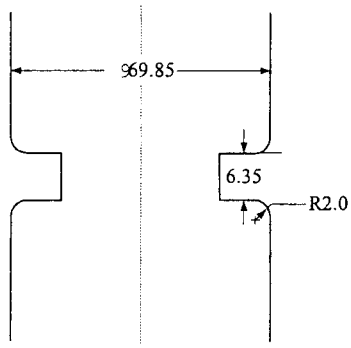

Fig. 4. Configuration of mandrel.

radii of main roll and guide roll are 114.3 and 25 mm, respectively. The configuration of mandrel is shown in Fig. 4. The friction coefficient is 0.2 on the main roll-ring interface, 0.1 on the mandrel-ring interface to fill the groove well and zero on the guide roll-ring interface. The total feed amount is 13.46 mm. Because the ring and forming rolls are initially symmetric in the axial direction, it is sufficient to view the problem as symmetric in this direction, and only half part of ring blank is considered to save calculating time.

3.2 Determining the Range of $\bar{f}$ for Modeling

In cold ring rolling process, only when the ith revolution feed amount Δh_i meets the following expression can the process proceed successfully [8].

$$\Delta h_{\min\_i} \le \Delta h_i \le \Delta h_{\max\_i}, (i = 1,2,3,\cdots,N). \quad (9)$$

where $\Delta h_{\min\_i}$ is the permissive minimum feed amount in the ith revolution by which the material in the roll gap can entirely come into plastic deformation state, and $\Delta h_{\max\_i}$ is the permissive maximum feed amount allowing the ring blank to be nipped into the roll gap continuously in the ith revolution. They can be calculated as follows [8]:

$$\Delta h_{\min\_i} = 6.55\times10^{-3}(R_i - r_i)^2\left(\frac{1}{R_D}+\frac{1}{R_M}+\frac{1}{R_i}-\frac{1}{r_i}\right),$$
$$(i = 1,2,3,\cdots,N). \quad (10)$$

$$\Delta h_{\max\_i} = \frac{2\beta^2 R_D}{(1+R_D/R_M)^2}\left(1+\frac{R_D}{R_M}+\frac{R_D}{R_i}-\frac{R_D}{r_i}\right),$$
$$(i = 1,2,3,\cdots,N). \quad (11)$$

For the case that the feed rate of mandrel is constant, the process can proceed successfully if the following two expressions are satisfied [8].

$$\Delta h_1 \ge \Delta h_{\min\_1}. \quad (12)$$

$$\Delta h_N \le \Delta h_{\max\_N}. \quad (13)$$

Combining Eqs. (4), (12) and (13), we can have

$$\frac{R_D \Delta h_{\min\_1}}{R_0} \le \frac{f}{n_1} \le \frac{R_D \Delta h_{\max\_N}}{R_{N-1}}. \quad (14)$$

Because $R_{N-1} \le R_N$, the value of $\bar{f}$ can be approximately determined by

$$\frac{R_D \Delta h_{\min\_1}}{R_0} \le \bar{f} \le \frac{R_D \Delta h_{\max\_N}}{R_N}. \quad (15)$$

When the total feed amount is 13.46 mm, the range of $\bar{f}$ is [0.2046, 2.0314] mm/rev according to Eqs. (10), (11) and (15).

4. The interactive influences of f and n_1 on T-shaped cold ring rolling process

4.1 The influence of f and n_1 on the process when $\bar{f}$ is changeless

4.1.1 Calculating conditions.

Here, f and n_1 are increased proportionally to keep $\bar{f}$ (*i.e.* f/n_1) unchanged. According to the range of $\bar{f}$, three cases, i.e. $\bar{f}$ = {0.2413, 0.4826, 0.9652} (mm/rev), are investigated. The corresponding values of f and n_1 are listed in Table 1, where A1 to A5 represent the five groups of values of f and n_1 when $\bar{f}$=0.2413 (mm/rev), B1 to B5 for the case when $\bar{f}$=0.4826 (mm/rev) and C1 to C5 for the case when $\bar{f}$=0.9652 (mm/rev).

Table 1. Values of f and n_1.

Parameter	$\bar{f}$ = 0.2413(mm/rev)					$\bar{f}$ = 0.4826(mm/rev)					$\bar{f}$ = 0.9652(mm/rev)				
	A1	A2	A3	A4	A5	B1	B2	B3	B4	B5	C1	C2	C3	C4	C5
f [mm/s]	0.623	0.935	1.247	1.87	2.493	0.62	0.94	1.25	1.87	2.49	0.62	0.94	1.25	1.87	2.49
n_1 [rev/s]	2.583	3.875	5.166	7.75	10.332	1.29	1.94	2.58	3.88	5.17	0.65	0.97	1.29	1.94	2.58

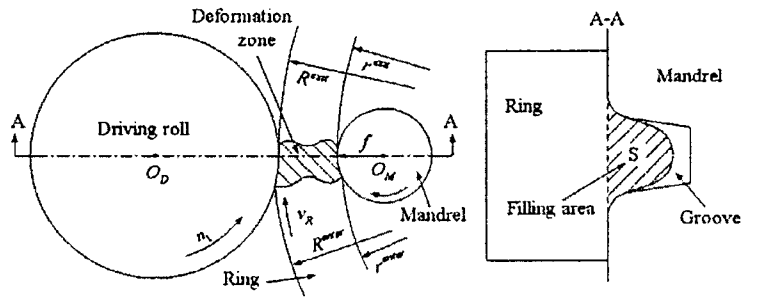

Fig. 5. The definition of filling area of groove.

4.1.2 *Influences of f and n_1 on RF, $\Delta\dot{R}$, φ_{id}, S, $\bar{B}$ and FT when $\bar{f}$ is unaltered*

Here, $\Delta\dot{R}$ is defined as $\Delta\dot{R} = (R - R_0)/R_0 \times 100\%$, it can measure the growing degree of ring diameter; φ_{id} is defined as $\varphi_{id} = \bar{\varepsilon}_{\max} - \bar{\varepsilon}_{\min}$, it can measure the inhomogeneous deformation of deformed ring; S is defined as the area of the metal filling into the groove on the section A-A at the rolling gap, as shown in Fig. 5, it can measure the filling capability of groove; $\bar{B}$ is defined as $\bar{B} = (B_{\max} + B_{\min})/2$, it can measure the metal magnitude flowing to the axial direction; FT is defined as $FT = (B_{\max} - B_{\min})/b_0 \times 100\%$, it directly reflects the quality of the end-plane of deformed ring.

The results of RF, $\Delta\dot{R}$, S, φ_{id}, $\bar{B}$ and FT in three cases above are listed in Table 2(a), (b) and (c), respectively. Here ξ_{RF}, $\xi_{\Delta\dot{R}}$, ξ_S, $\xi_{\varphi_{id}}$, $\xi_{\bar{B}}$ and ξ_{FT} defined as follows are adopted to measure the change rates of RF, $\Delta\dot{R}$, S, φ_{id}, $\bar{B}$ and FT, respectively.

$$\xi_{RF} = \left(RF_{\max} - RF_{\min}\right)/RF_{\min} \times 100\%;$$

$$\xi_{\Delta\dot{R}} = \Delta\dot{R}_{\max} - \Delta\dot{R}_{\min};$$

$$\xi_{\varphi_{id}} = \left(\varphi_{id\max} - \varphi_{id\min}\right)/\varphi_{id\min} \times 100\%;$$

$$\xi_S = \left(S_{\max} - S_{\min}\right)/S_{\min} \times 100\%;$$

$$\xi_{\bar{B}} = \left(\bar{B}_{\max} - \bar{B}_{\min}\right)/b_0 \times 100\%;$$

$$\xi_{FT} = FT_{\max} - FT_{\min}.$$

Table 2(a). The results of studying objects when $\bar{f}$ = 0.2413 (mm/rev).

	A1	A2	A3	A4	A5	ξ
RF (KN)	39.12	38.48	38.36	38.61	37.97	*3.03%*
$\Delta\dot{R}$ (%)	30.33	30.53	30.48	30.46	30.48	*0.20%*
φ_{id}	2.199	2.158	2.172	2.192	2.177	*1.93%*
S (mm^2)	33.61	33.50	33.23	33.48	33.42	*1.13%*
$\bar{B}$ (mm)	15.27	15.24	15.22	15.44	15.32	*0.86%*
FT (%)	*28.16*	*28.01*	*28.05*	*28.49*	*28.18*	*0.49%*

Table 2(b). The results of studying objects when $\bar{f}$ = 0.4826 (mm/rev).

	B1	B2	B3	B4	B5	ξ
RF (KN)	45.53	45.33	45.34	45.92	46.01	*1.5%*
$\Delta\dot{R}$ (%)	33.99	34.56	34.70	34.74	34.76	*0.77%*
φ_{id}	1.987	1.933	1.895	1.893	1.901	*4.37%*
S (mm^2)	30.78	30.17	30.25	30.19	30.23	*2.02%*
$\bar{B}$ (mm)	13.24	12.76	12.67	12.66	12.73	*4.25%*
FT (%)	*26.60*	*24.28*	*24.15*	*24.16*	*23.89*	*4.01%*

Table 2(c). The results of studying objects when $\bar{f}$ = 0.9652 (mm/rev).

	C1	C2	C3	C4	C5	ξ
RF (KN)	52.24	51.79	51.95	52.53	51.94	*1.43%*
$\Delta\dot{R}$ (%)	37.23	37.40	37.95	38.73	38.72	*1.50%*
φ_{id}	1.832	1.814	1.787	1.756	1.756	*4.37%*
S (mm^2)	29.32	30.06	29.69	29.16	29.85	*3.22%*
$\bar{B}$ (mm)	10.57	10.59	10.31	9.82	9.82	*3.07%*
FT (%)	*23.46*	*23.24*	*22.25*	*20.63*	*20.51*	*2.95%*

It can be obtained that all of the change rates of RF, $\Delta\dot{R}$, φ_{id}, S, $\bar{B}$ and FT are less than 5 %. So it can be considered that, whatever f and n_1 change, RF, $\Delta\dot{R}$, φ_{id}, S, $\bar{B}$ and FT are approximately unchanged as long as $\bar{f}$ is unaltered.

4.2 The influence of $\bar{f}$ on the process

4.2.1 Calculation conditions.

In this paper, {0.2413, 0.2896, 0.3620, 0.4826, 0.7239, 0.9652} (mm/rev) are selected as the values of $\bar{f}$ by using the following two approaches to investigate the effects of $\bar{f}$ on RF, $\Delta\dot{R}$, φ_{id}, S, $\bar{B}$ and FT.

The first approach: order n_1 =2.583 (rev/s), then select f = {0.623, 0.748, 0.935, 1.247, 1.870, 2.493} mm/s correspondingly;

The second approach: order f =1.267 (mm/s), then select n_1 = {5.166, 4.306, 3.444, 2.583, 1.722, 1.292} (rev/s) correspondingly.

4.2.2 Variations of RF, $\Delta\dot{R}$, S, φ_{id}, $\bar{B}$ and FT.

The variations of RF, $\Delta\dot{R}$, φ_{id}, S, $\bar{B}$ and FT with $\bar{f}$ are illustrated in Figs. 6-11, respectively, where the real line with hollow circle represents the first approach, while the broken line with solid circle stands for the second one. From the Figs. 6-11, it can be seen that the variational curve with $\bar{f}$ of each object obtained by the first approach is approximately similar to that obtained by the second one. With the increase of $\bar{f}$, RF and $\Delta\dot{R}$ increase gradually while φ_{id}, S, $\bar{B}$ and FT decrease rapidly first and then slowly. This is because the increase of $\bar{f}$ results in the increase of Δh. Therefore, the deforming metal per roll time increases causing the roll force to increase. Meanwhile, with the increase of Δh, the plastic deformation zone gradually penetrates the thickness of ring, the constraint of the circumferential elongation enforced by the metal near the medium radius decreases. Thus, $\Delta\dot{R}$ increases while φ_{id}, S, $\bar{B}$ and FT decrease. When Δh increases to the value at which the plastic deformation zone has already penetrated thoroughly through the thickness of ring, the metal in the roll gap deforms very uniformly, so $\Delta\dot{R}$, φ_{id}, S, $\bar{B}$ and FT change slowly with the increase of Δh, especially for S.

From Figs. 6-11, it can also be seen that the

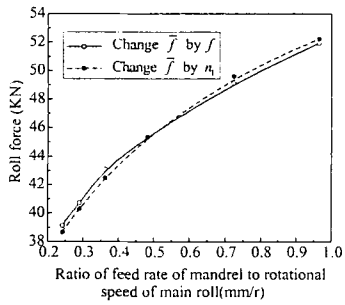

Fig. 6. Variation of roll force.

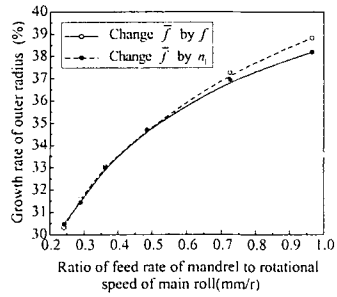

Fig. 7. Variation of growth rate of outer d iameter.

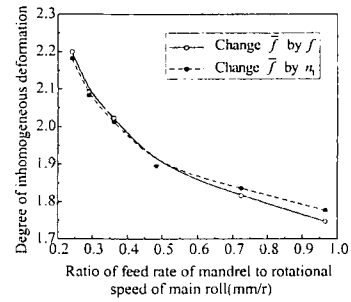

Fig. 8. Variation of degree of inhomogeneous deformation.

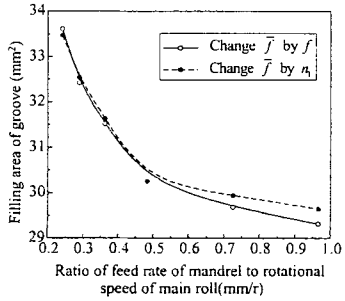

Fig. 9. Variation of filling area.

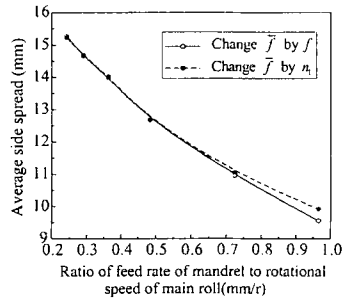

Fig. 10. Variation of side spread.

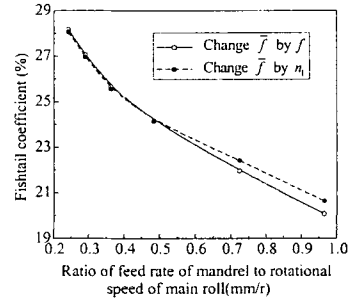

Fig. 11. Variation of fishtail coefficient.

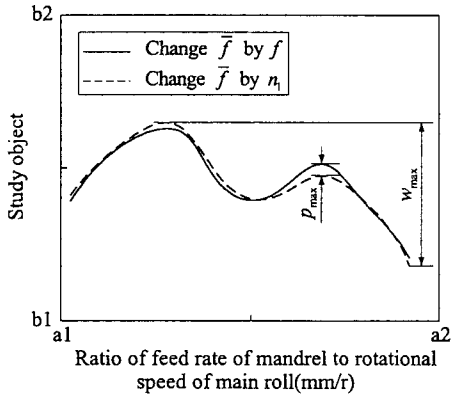

Fig. 12. Definition for p_{max} and w_{max} .

differences between the two curves of each object among RF, $\Delta\dot{R}$, φ_{id}, S, $\bar{B}$ and FT are very little when $\bar{f}$ is less than 0.4826 mm/rev; but when $\bar{f}$ exceeds 0.4826 mm/rev, the difference increases gradually if $\bar{f}$ increased continuously. In this paper, $\zeta = p_{max} / w_{max}$ is adopted to measure the discrepancy between two curves in the same coordinate system, where p_{max} and w_{max} are shown in Fig. 12, and their definitions are as follows:

$$p_{max} = \max\left\{\left|y_1(\bar{f}) - y_2(\bar{f})\right|\right\}$$

$$w_{max} = \min\left\{\left[\max(y_1(\bar{f}) - \min(y_1(\bar{f}))\right], \left[\max(y_2(\bar{f}) - \min(y_2(\bar{f}))\right]\right\},\ \bar{f} \in [\bar{f}_1, \bar{f}_2].$$

where $y_1(\bar{f})$ and $y_2(\bar{f})$ are the curves changing with $\bar{f}$, the subscript 1 represents that $\bar{f}$ is changed by f and subscript 2 represents that $\bar{f}$ is changed by n_1. The ζ of RF, $\Delta\dot{R}$, φ_{id}, S, $\bar{B}$ and FT are 5.97 %, 8.26 %,7.41 %, 8.60 %, 6.80 % and 7.65 %, respectively. Thus it can be considered that the two curves of each object are approximately similar. It can be concluded that increasing (decreasing) f or decreasing (increasing) n_1 can achieve the identical effect in the cold ring rolling process.

5. Conclusions

The interactive influences f and n_1 on RF, $\Delta\dot{R}$, φ_{id}, S, $\bar{B}$ and FT in T-shaped cold ring rolling process are revealed. The following conclusions can be drawn.

(1) Whatever f and n_1 change, RF, $\Delta\dot{R}$, φ_{id}, S, $\bar{B}$ and FT are nearly unchanged under the condition that $\bar{f}$ is changeless;

(2) The variational curve of RF changing with $\bar{f}$ when $\bar{f}$ is changed by f is approximately the same as the one when $\bar{f}$ is changed by n_1, so are $\Delta\dot{R}$, φ_{id}, S, $\bar{B}$ and FT. Thus, by increasing (decreasing) f or decreasing (increasing) n_1, the identical effect can be obtained in the process;

(3) The increase of $\bar{f}$ is favourable to the growth of $\Delta\dot{R}$ and the restriction of φ_{id}, $\bar{B}$ and FT, but it causes RF to increase and S to decrease.

Acknowledgements

The authors wish to thank the Natural Science Foundation for Key Program of China (No. 50335060) and the Natural Science Foundation of China for Distinguished Young Scholars (No. 50225518) for the support given to this research.

Nomenclature

Δh : feed amount per revolution of ring
Δh_i, Δt_i : thickness reduction and roll time in the ith revolution of ring
R_i, r_i, H_i : outer, inner radii and thickness of ring in the ith revolution of ring, respectively
R_0, r_0, H_0 b_0 : outer radius, inner radius, thickness and axial width of ring blank, respectively
v_R, v_D : linear velocity of the outer circle of ring blank and main roll, respectively
R_M, R_D, R : radius of mandrel, main roll and deformed ring, respectively
f, n_1 : feed rate of mandrel and rotational speed of main roll, respectively
$\bar{f}$: the ration of feed rate of mandrel to rotational speed of main roll
β : friction angle
RF, S : roll force and filling area of groove, respectively
φ_{id}, $\Delta\dot{R}$: degree of inhomogeneous deformation and growth rate of radius, respectively

$\bar{B}$, FT : average side spread and fishtail coefficient of deformed ring, respectively

B_{max}, B_{min} : maximum and minimum axial side spread of deformed ring, respectively

$\bar{\varepsilon}_{max}$, $\bar{\varepsilon}_{min}$: maximum and minimum equivalent plastic strain of deformed ring, respectively

Reference

[1] A. G. Mamalis, J. B. Hawkyard, Johnson, Spread and flow patterns in ring-rolling, *Int. J. Mech. Sci.* 18(1),(1976) 11-16.

[2] J. B. Hawkyard, W. Johnson, J. Kirkland, E. Appleton, Analyses for roll force and torque in ring rolling with some supporting experiments, *Int. J. Mech. Sci.* 15 (1973) 873-893.

[3] C. F. Lugora and A. N. Bramley, Analysis of spread in ring-rolling. *Int. J. Mech. Sci.* 29 (1987) 149-157.

[4] N. Kim, S. Machida, S. Kobayashi, Ring rolling process simulation by the three dimensional finite element method. *Int. J. Mach. Tools Manuf.* 30 (1990) 569-577.

[5] L. G. Guo, H. Yang and M. Zhan, Research on plastic deformation behaviour in cold ring rolling by FEM numerical simulation, *Modelling Simul. Mater. Sci. and Eng.* 13 (2005) 1029-1046.

[6] H. Yang, L. G. Guo, M. Zhan and Z. C. Sun, Research on the influence of material properties on cold ring rolling process by 3D-FE numerical simulation, *J. Mater. Process. Technol.* 177 (2006) 634-638.

[7] Z. W. Wang, S. Q. Zeng, X. H. Yang and C. Cheng, The key technology and realization of virtual ring rolling, *J. Mater. Process. Technol.* 182 (2007) 374-381.

[8] L. Hua, X. G. Huang and C. D. Zhu, Theory and Technology of the Ring Rolling. China Mechanical Industry Press, Beijing, (2001).

[9] L. Y. Li, H. Yang, L. G. Guo and Z. C. Sun, A Control Method of Guide Rolls in 3D-FE Simulation of Ring Rolling. *J. Mater. Process. Technol.* (accepted).